Rapid and Specific Targeting of ^{125}I-Labeled B Lymphocyte Stimulator to Lymphoid Tissues and B Cell Tumors in Mice

Todd A. Riccobene, PhD[1]; Renée C. Miceli, MEd[1]; Clint Lincoln[1]; Yvonne Knight;[1] Joseph Meadows, BA[1]; Michael G. Stabin, PhD[2]; and Cynthia Sung, PhD[1]

[1]*Preclinical Development, Human Genome Sciences, Incorporated, Rockville, Maryland; and* [2]*Department of Radiology and Radiological Sciences, Vanderbilt University, Nashville, Tennessee*

B lymphocyte stimulator (BLyS) protein is a member of the tumor necrosis factor (TNF) superfamily of cytokines that binds to B lineage cells, but not T cells, monocytes, natural killer cells, or granulocytes. BLyS protein binding to B cells is restricted to immunoglobulin-positive cells and is not evident on pro- or pre-B cell populations. This unique binding profile suggests that a radiolabeled form of BLyS protein may be a useful treatment for B cell neoplasias such as B cell lymphoma and multiple myeloma. Here, we report the biodistribution of radiolabeled recombinant human BLyS after intravenous injection into normal mice and mice bearing BCL1 tumor in the spleen or J558 tumor in the subcutaneous space. We also report the use of these data to estimate human dosimetry. **Methods:** ^{125}I-Labeled BLyS protein (50 μg/kg, 0.185–0.37 MBq per mouse) was injected intravenously into BALB/c mice, and biodistribution was measured by direct counting of radioactivity in dissected tissues and by quantitative whole-body autoradiography (QWBA). **Results:** The half-life of radiolabeled BLyS protein in blood was ~2.7 h in both normal and tumor-bearing mice. The spleen showed the highest uptake of BLyS protein in both normal and tumor-bearing mice, with a maximum concentration (C_{max}) of 35–45 percentage injected dose per gram (%ID/g) occurring between 1 and 3 h after injection. In lymph nodes, C_{max} was ~20 %ID/g in normal and J558 tumor-bearing mice and 8–15 %ID/g in BCL1 tumor-bearing mice. Limited biodistribution data from the J558 tumors showed a C_{max} of ~15 %ID/g. By contrast, C_{max} was only ~5 %ID/g for both kidney and liver. QWBA confirmed high radioactivity in spleen, lymph nodes, and stomach contents and low radioactivity in kidney and liver. After 24 h, spleen and lymph nodes were still positive in QWBA images, whereas liver and kidney no longer had observable levels. **Conclusion:** Radiolabeled BLyS showed specific and rapid targeting to lymphoid tissues and B cell tumors in mice. Unlike monoclonal antibodies, which have long plasma half-lives and considerable liver uptake, BLyS has distinct pharmacokinetic and biodistribution properties that may offer advantages compared with antibody-based radioimmunotherapy.

Key Words: biodistribution; radiolabeled BLyS protein; B cell neoplasia

J Nucl Med 2003; 44:422–433

B lymphocyte stimulator (BLyS protein, also known as BAFF (B cell activating factor belonging to the tumor necrosis factor [TNF] family), TALL-1 (TNF and apoptosis ligand-related leukocyte-expressed ligand 1), zTNF4, TNFS20 (TNF superfamily member 20), or THANK (TNF homologue that activates apoptosis, nuclear factor [NF]-κB, and c-Jun NH_2-terminal kinase) is a member of the TNF superfamily of cytokines that was first identified from a human neutrophil/monocyte-derived complementary DNA library. BLyS shares homology with other ligands in the TNF family, including APRIL (a proliferation-inducing ligand), TNFα, lymphotoxin-α, and TRAIL (TNF-related apoptosis-inducing ligand). Full-length BLyS is a 285–amino acid type II transmembrane protein with a carboxy terminal extracellular domain and, like other TNF ligands, is cleaved to form a soluble product. Highest levels of full-length BLyS messenger RNA have been found in spleen, lymph nodes, bone marrow, peripheral blood mononuclear cells, and myeloid cell lines (*1*).

A soluble form of BLyS has been produced in both prokaryotic and eukaryotic expression systems (*1–4*). This recombinant human BLyS consists of 152 amino acids and forms a 52-kDa homotrimer in solution (*1*). BLyS protein is known to promote B cell proliferation, activation, and differentiation, enhance B lymphocyte survival, and thereby stimulate immunoglobulin production both in vitro and in vivo (*1–6*). In normal mice receiving injections of BLyS, lymphoid compartments in the spleen undergo marked expansion, and plasma levels of immunoglobulins increase significantly (*7*). The role of BLyS in B cell homeostasis became evident from studies in BLyS null (*8*,*9*) and BLyS

Received Mar. 25, 2002; revision accepted Jul. 26, 2002.
For correspondence or reprints contact: Todd A. Riccobene, PhD, Human Genome Sciences, Inc., 9410 Key West Ave., Rockville, MD 20850.
E-mail: todd_riccobene@hgsi.com

transgenic mice (*10–12*). Mice lacking BLyS have extreme reductions of mature B cells in peripheral blood, whereas mice overexpressing BLyS have increased numbers of mature splenic and lymph node B cells, elevated immunoglobulin levels, and manifestations of autoimmune disease.

Three cellular receptors that bind BLyS with similar high affinities have been identified: transmembrane activator and calcium-modulating cyclophilin ligand interactant (TACI), B cell maturation antigen (BCMA), and BAFF-receptor/BLyS receptor 3 (BAFF-R) (*12–20*). BAFF-R and BCMA expression is restricted to B cells, whereas TACI is found on both B cells and activated T cells. The BLyS receptors appear to be expressed on immunoglobulin-positive B cells but not on immunoglobulin-negative pre- and pro-B cells. In vitro studies have determined that radiolabeled BLyS binding to human tonsillar B cells is specific and saturable, with a dissociation constant of 0.1 nmol/L and approximately 2,600 binding sites per cell (*21*).

BLyS receptors are expressed on a broad range of tumor cells of B cell lineage, including multiple myeloma, large B cell lymphoma, follicular B cell lymphoma, chronic lymphocytic leukemia, and Burkitt's lymphoma (*22*). This receptor distribution suggests that BLyS has significant potential as a targeting protein for an extensive array of B cell malignancies. Because of the radiosensitivity of these types of tumors, BLyS labeled with a cytotoxic radionuclide may be able to deliver a sufficient radiation dose to induce tumor cell death.

Recently, it has been demonstrated that radioimmunotherapy with monoclonal antibodies directed against the B cell–specific CD20 antigen achieves significant response rates in non-Hodgkin's lymphoma (*23*,*24*). One drawback of this therapy is the substantial radiation dose delivered to normal organs from the circulating, long–half-lived monoclonal antibody. This limits the dose that can be given to the patient and may contribute to the tumor relapses seen after initial positive responses. Binding of radiolabeled anti-CD20 antibodies on pre-B cells may also lead to delayed rebound of mature lymphocytes. In addition, the CD20 antigen is expressed on the malignant plasma cells of only about 20% of multiple myeloma patients (*25*). BLyS, in contrast, binds to multiple myeloma cells, does not bind to early pre- and pro-B cells, and has a much shorter half-life in mice than immunoglobulins (half-life of 2.7 h, compared with 4–5.4 d for IgG (*7*,*26*)). These characteristics may allow BLyS to be used in clinical situations as an alternative to monoclonal antibody radioimmunotherapy.

The following biodistribution studies in normal and tumor-bearing mice provide quantitative in vivo data on the localization and clearance of radiolabeled BLyS. Direct γ-counting of dissected tissues and quantitative whole-body autoradiography (QWBA) indicate that ^{125}I-BLyS preferentially binds to tissues with high concentrations of B lymphocytes such as spleen, lymph nodes, marrow, gut-associated lymphoid tissue, B cell lymphomas, and plasma cell tumors. Uptake of ^{125}I-BLyS was rapid and specific. In contrast, tissues with nonspecific uptake such as kidney and liver were quickly cleared of radioisotope. These studies confirm the targeting potential of radiolabeled BLyS. The restricted expression patterns of BLyS receptors together with the pharmacokinetic profile and favorable distribution of radiolabeled BLyS support the further development of radiolabeled BLyS as a potentially novel treatment for B cell disease.

MATERIALS AND METHODS

Radiolabeling

Recombinant human BLyS was produced at Human Genome Sciences, Inc. (Rockville, MD), in *Escherichia coli* as a soluble 52-kDa trimeric protein. BLyS was labeled with ^{125}I at MDS Nordion (Kanata, Ontario) using a method of iodination that directly modifies tyrosine residues on the protein. The specific activity of ^{125}I-BLyS was 263–287 MBq/mg (7.10–7.75 mCi/mg) BLyS, the BLyS concentration was 0.4 mg/mL, and the molar ratio of iodine to BLyS was 1.74–1.90. Before injection, ^{125}I-BLyS was diluted to a concentration of 5 μg/mL in buffer (10 mmol/L sodium citrate, 140 mmol/L NaCl, pH 6.0). The percentage of free iodine (measured by trichloroacetic acid [TCA] precipitation) in the dosing solutions administered to animals used for determining biodistribution ranged from 15% to 18%.

Animals and Dosing

Female BALB/c mice 10–12 wk old weighing from 20 to 24 g were obtained from Ace Animals (Boyertown, PA) and allowed to acclimate for at least 1 wk before the start of the experiment. Three to 5 d before the start of the experiment, and continuing up to the time of sacrifice, mice were given drinking water containing 0.4% Lugol's solution (Sigma) to block thyroid uptake of ^{125}I. Fifteen days before injection with ^{125}I-BLyS, mice designated to receive the BCL1 tumor were injected intraperitoneally with 3×10^5 viable BCL1 cells. Mice selected to receive the J558 tumor were injected subcutaneously above the right hind limb with 5×10^5 viable J558 cells 10 d before injection with ^{125}I-BLyS.

Mice were injected intravenously through the tail vein with 0.01 mL/g of body weight at 5 μg/mL, to give a final protein dose of 50 μg/kg ^{125}I-BLyS (0.185–0.37 MBq per mouse). At the specified time after injection (1, 3, 16, or 24 h), mice were euthanized by CO_2 overexposure, and a urine sample was collected. Mice were designated for either tissue dissection or QWBA to determine biodistribution. In addition, for a more complete description of the blood and plasma curves for ^{125}I-BLyS, 3 mice per time point were sacrificed at 5 and 30 min after injection and only blood, plasma, and urine were taken.

Biodistribution

After sacrifice, the animals that were designated for dissection were exsanguinated through the inferior vena cava, and the blood was transferred to tubes containing ethylenediaminetetraacetic acid (0.78 mg per tube; Termuno Medical Corp., Elkton, MD). An aliquot of whole blood was taken for γ-counting and the remaining blood was centrifuged to obtain plasma. Plasma and whole blood were read on the γ-counter before and after TCA precipitation. The following tissues were removed, weighed, and counted on a γ-counter: spleen, mesenteric lymph node, kidney, part of the liver, stomach, part of the duodenum, heart, lung, a piece of skeletal muscle (biceps femoris), and part of the femur.

QWBA

Mice designated for QWBA were euthanized with CO_2, positioned onto a metal plate, and frozen in a slurry of dry ice and isopentane. Limbs were removed from the frozen carcass, and the carcass was decapitated. Body and head were embedded separately in optimal cutting temperature (OCT) compound (Sakura Finetek, Torrance, CA). The embedded blocks were stored at −80°C until the time of sectioning, when they were mounted on a cryostat (Carl Zeiss Inc., Thornwood, NY) maintained at −20°C. Sections were obtained by placing plastic adhesive tape on the block and cutting 20-μm sections through the block. Sections from the bodies were made at 2-mm intervals starting from the level of the spleen, and sections from the head were made at 1-mm intervals starting at the orbit of the eye. The sections used for autoradiography were left on the tape and placed in plastic sleeves for protection. Corresponding sets of adjacent sections were transferred to glass slides coated with a photo-cross-linkable polymer gel, briefly exposed to ultraviolet light, and stained with hematoxylin and eosin (H&E).

To quantify the amount of radioactivity per gram of tissue from the QWBA sections, tissue standards were prepared by adding a known amount of ^{125}I to BALB/c mouse liver homogenate. Liver homogenates were then placed into holes drilled in a block of OCT compound, frozen, and cut into 20-μm sections for the standards. QWBA sections were exposed to previously erased imaging plates (Fuji Photo Film Co., Tokyo, Japan) inside a cassette along with the ^{125}I tissue standards. After exposure, the imaging plates were read on a BAS-2500 IP reader (Fuji Photo Film Co.). Images from the IP reader were quantified with Image Gauge software (version 3.0; Fuji Photo Film Co.). Regions corresponding to organs and tissues were selected on the basis of structures identified on adjacent H&E-stained sections.

TCA Precipitation and γ-Counting

The percentage of protein-bound radioactivity in the ^{125}I-BLyS dosing solution, urine, plasma, and whole blood was determined by TCA precipitation. Samples were read on the γ-counter, then 200 μL of 5% bovine serum albumin were added to the sample followed by 200 μL of 12% TCA. The samples were then stirred and incubated at 4°C for 10 min. After incubation, the samples were centrifuged, the supernatant was removed by aspiration, and the samples were recounted on the γ-counter.

Counts per minute (CPM) in dissected tissues, blood, plasma, urine, and dosing solutions were determined using a γ-counter (Wallac 1480 WIZARD; Perkin Elmer Life Sciences Inc., Boston, MA). The counter subtracts background and calculates an adjusted CPM. The adjusted CPM was then used to calculate percentage injected dose per gram of tissue (%ID/g) or milliliter of fluid (%ID/mL) and the percentage of TCA-precipitable radioactivity. The %ID/g was calculated by dividing the adjusted CPM by the tissue weight and the CPM injected for that animal. The %ID/mL was calculated by dividing the adjusted CPM by the fluid volume and the CPM injected for that animal. The ratio of CPM before and after TCA precipitation (×100) was taken as the percentage of protein-bound radioactivity.

Dosimetry

Dose estimate tables for BLyS labeled with ^{131}I were developed on the basis of biodistribution data from tissue dissection and QWBA in normal 20-g BALB/c mice using the ^{125}I-labeled compound. Data for the %ID/g in the animal organs were extrapolated to humans using the approach of Kirschner et al. (*27*), which assumes that the %ID/g normalized by the whole body weight, in kilograms (i.e., the %ID-kg/g), is the same in the animal and the human. In addition, the time scale was extrapolated according to the ratio of the human-to-animal total-body masses raised to the 0.25 power (*28*). Data were fit with SAAM II software (SAAM Institute, Inc., Seattle, WA) using 1 or 2 exponential functions. From the fitted functions, organ residence times were estimated. Activity not accounted for in any organ was assigned to the remainder of the body and assumed to clear the body with the total-body clearance kinetics. Data from the lymph system were not used directly. This activity was assumed to be part of the "remainder of the body" for dosimetry purposes. The total-body retention data were assumed to give the best estimate of the excretion of the compound. For most organs, the fitted biokinetic model was represented as an initial fractional uptake and a biologic half-time. In all cases except the thyroid, the functions were derived as $\Sigma\, a_i \times \exp(-\lambda_i t)$ (with either 1 or 2 terms). In the case of thyroid, the functional form was $a_i \times (1 - \exp[-\lambda_i t])$. Dose estimates were calculated using the MIRDOSE3.1 computer program (*29*).

RESULTS

Biodistribution in Normal Mice

The %ID/g of ^{125}I-BLyS at 1, 3, 6, 16, and 24 h after injection into normal mice is shown in Figure 1 for the tissues collected by dissection. The highest %ID/g among these tissues (which did not include thyroid) was found in the spleen (maximum concentration [C_{max}] = 45.2). High levels were also found in the mesenteric lymph nodes (C_{max} = 17.7). This localization agrees with the expression of BLyS receptors, found predominantly on mature, immunoglobulin-positive B cells. The high levels of radioactivity found in the stomach (C_{max} = 25.7) are consistent with the known elimination routes of free iodine (*30*). High levels of radioactivity in the lung (C_{max} = 27.2) may be associated with ^{125}I-BLyS in the blood in this highly perfused tissue, and ^{125}I-BLyS clears from the lung with a half-life similar to the plasma half-life. The kidneys, liver, muscle, heart, duodenum, and femur all had relatively low %ID/g.

The %ID/mL values for blood, plasma, and urine (TCA-precipitable activity) are listed in Table 1. The plasma half-life of ^{125}I-BLyS in BALB/c mice is 2.7 h, a value comparable to that of unlabeled BLyS in BALB/c mice (*7*). The percentage TCA-precipitable (protein bound) radioactivity in the plasma is comparable to that of the dose solution for 3 h after injection (76%–89%) but decreases significantly to 52%–55% by 6 h after injection. The time course of the increase in nonprotein-bound radioactivity in the circulation parallels the accumulation of radioactivity in the stomach, further supporting the presence of free ^{125}I in the stomach. Little of the radioactivity in the urine is precipitable by TCA (~5%), consistent with dehalogenation of the BLyS protein, or degradation of BLyS into small peptides or amino acids.

The ratios of the area under the %ID/g curve (AUC) for the tissues (AUC_{tissue}) to that in the blood (AUC_{blood}) are

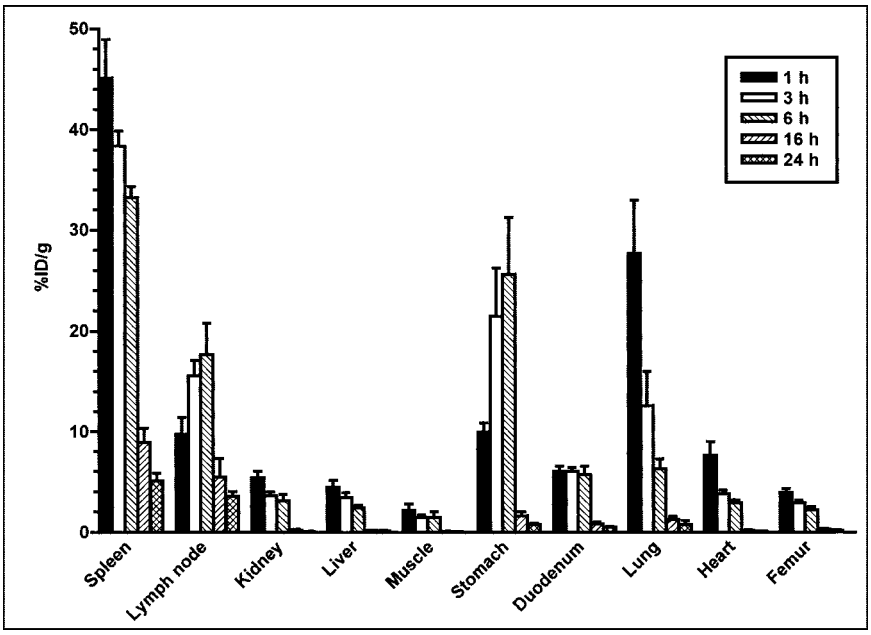

FIGURE 1. %ID/g after intravenous injection of 50 μg/kg of ^{125}I-BLyS into normal BALB/c mice. Female BALB/c mice were injected intravenously with ^{125}I-BLyS at 50 μg/kg, and biodistribution was determined by the tissue dissection method at 1, 3, 6, 16, and 24 h after injection. Error bars represent SEM.

listed in Table 2. Spleen and lymph node had the highest AUC_{tissue}/AUC_{blood}, with values of 6.53 and 3.35, respectively. In contrast, the AUC ratios for the lung, kidney, and liver were 1.65, 0.50, and 0.42, respectively, demonstrating greater specificity of ^{125}I-BLyS for lymphoid tissues. The stomach also had a high AUC ratio (3.16), presumably because of free ^{125}I.

QWBA images for normal mice are shown in Figure 2. The images confirm the localization of ^{125}I-BLyS to the spleen and lymph nodes and also demonstrate targeting to gut-associated lymphoid tissue. By comparison, kidney and liver have low levels of radioactivity, and by 16 h, lung, kidney, and liver are not visible in the images. High levels of radioactivity are also found in the thyroid (not shown), stomach, and submandibular salivary gland, consistent with the expected distribution of free iodine (*30*). High radioactivity in the thyroid indicates that blocking with Lugol's solution was incomplete. Examination of adjacent H&E-stained sections shows that the radioactivity in the stomach appears to be in the luminal contents, not concentrated in the stomach wall. Radioactivity is also found in the mineralized regions of the teeth. The mechanism for localization to teeth is not clear but could be related to the fact that teeth become permeable to iodide as they cycle through mineralization and demineralization (*31*).

The %ID/g values for various tissues are listed in Table 3. For comparison, the values for %ID/g determined by tissue dissection are also listed in Table 3. Results obtained for the 2 techniques are quite comparable, although each method is associated with different limitations. In QWBA, different tissues may undergo different thermal expansion during freezing, whereas in tissue dissection, loss of blood is greater from organs with high blood volume than from other organs. The QWBA technique has the advantage of being

TABLE 1
%ID (TCA-Precipitable)/mL of Blood, Plasma, and Urine After Intravenous Injection of 50 μg/kg of ^{125}I-BLyS into Normal BALB/c Mice (±SEM)

Time	Blood	Plasma	Urine
5 min	22.80 ± 1.28	48.20 ± 1.82	8.74
30 min	17.40 ± 1.51	40.90 ± 2.68	10.20 ± 2.27
1 h	9.45 ± 2.07	26.00 ± 3.95	6.06 ± 0.57
3 h	5.13 ± 0.85	10.50 ± 1.58	10.30 ± 3.60
6 h	2.32 ± 0.13	3.60 ± 0.34	6.69 ± 0.83
16 h	0.14 ± 0.04	0.11 ± 0.04	0.08 ± 0.14
24 h	0.08 ± 0.01	0.09 ± 0.01	0.74 ± 0.11

Urine values represent activity present only at specified time point, not cumulative excretion.

TABLE 2
Ratio of AUC_{tissue} to AUC_{blood} in Normal Mice

Tissue	AUC	AUC_{tissue}/AUC_{blood}
Blood	81.3	1.00
Spleen	531.0	6.53
Lymph node	272.0	3.35
Stomach	257.0	3.16
Lung	134.0	1.65
Duodenum	74.8	0.92
Heart	42.0	0.52
Kidney	40.2	0.50
Liver	34.1	0.42
Femur	32.0	0.39
Muscle	17.6	0.22

SOCIETY OF NUCLEAR MEDICINE

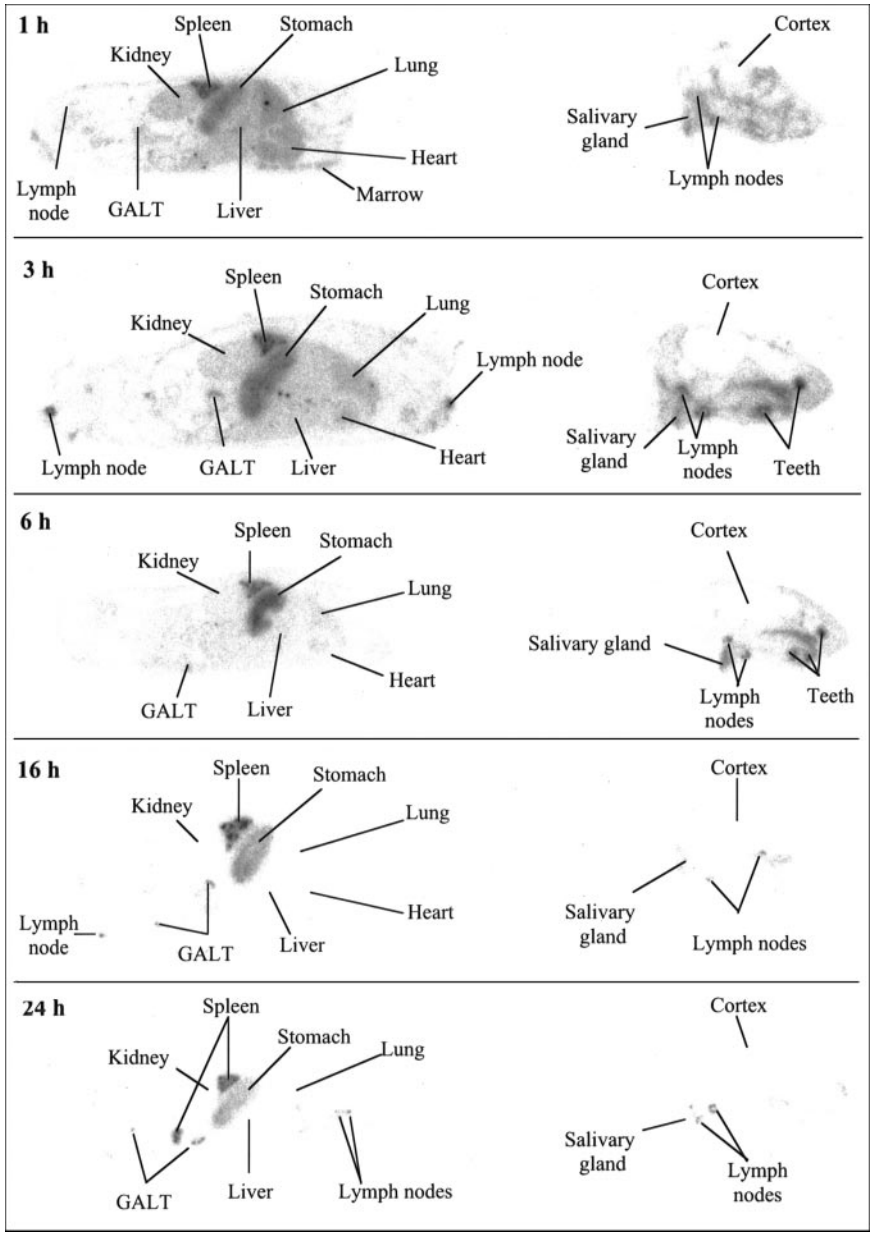

FIGURE 2. QWBA after intravenous injection of 50 μg/kg of ^{125}I-BLyS into normal BALB/c mice. Female BALB/c mice were injected intravenously with ^{125}I-BLyS at 50 μg/kg and were frozen for QWBA at 1, 3, 6, 16, and 24 h after injection. Images were contrast-enhanced for display purposes only. GALT = gut-associated lymphoid tissue.

able to detect accumulation in tissues not removed by dissection, and it can show spatial distributions within a particular organ. For example, in this study, we found that the gut-associated lymphoid tissue had a higher concentration of radioactivity than did other parts of the gut. The disadvantage of QWBA is that it is more labor- and time-intensive than the dissection method.

Biodistribution in BCL1 Tumor-Bearing Mice

The BCL1 line was derived from a spontaneous mouse B cell tumor (*32*). When BCL1 cells are injected intraperitoneally into BALB/c mice, splenomegaly and leukemia develop, and the splenic architecture is progressively disrupted by tumor cell infiltration and proliferation. The BCL1 tumor cell phenotype is IgM positive, is complement receptor negative, is Fc receptor positive, and has marginal IgD expression. Fluorescence-activated cell sorter analysis using biotinylated BLyS shows that BCL1 cells freshly isolated from the spleens of BALB/c mice express the BLyS receptors on their cell surface.

The spleens of mice 15 d after intraperitoneal injection of 3×10^5 BCL1 cells were noticeably enlarged, with an average weight of 194 ± 2.6 mg (mean ± SEM). This is significantly greater than the spleen weight of normal mice (80–100 mg) and is consistent with the known in vivo growth pattern of BCL1 cells.

The %ID/g of ^{125}I-BLyS in BCL1 tumor-bearing mice at 1, 3, 6, 16, and 24 h after injection is shown in Figure 3 for the tissues collected by dissection. The highest %ID/g was

TABLE 3
%ID/g Determined by Whole-Body Autoradiography or Tissue Dissection

Tissue	Biodistribution method	*n*	1 h	3 h	6 h	16 h	24 h
Spleen	Autoradiography	2	36.00	39.20	33.70	12.30	4.77
	Tissue dissection	3	39.10	34.40	28.50	10.40	6.25
	Mean	5	37.80	36.30	30.60	11.20	5.66
Lymph node	Autoradiography	2	9.30	17.40	13.60	4.16	2.51
	Tissue dissection	3	9.20	20.10	17.40	3.94	3.11
	Mean	5	9.24	19.00	15.90	4.03	2.87
Stomach	Autoradiography	2	7.99	16.60	14.20	1.87	1.33
	Tissue dissection	3	7.07	10.80	21.50	2.62	0.61
	Mean	5	7.44	13.10	18.60	2.32	0.90
Lung	Autoradiography	2	14.50	9.06	4.42	0.25	0.15
	Tissue dissection	3	17.00	7.70	3.89	0.35	0.17
	Mean	5	16.00	8.24	4.11	0.31	0.16
Duodenum	Autoradiography	2	3.45	5.67	5.95	0.57	0.38
	Tissue dissection	3	5.18	4.52	4.80	1.68	0.37
	Mean	5	4.49	4.98	5.26	0.64	0.38
Heart	Autoradiography	2	9.28	6.92	3.56	0.14	0.12
	Tissue dissection	3	7.49	3.72	2.03	0.15	0.07
	Mean	5	8.21	5.00	2.64	0.15	0.09
Kidney	Autoradiography	2	5.64	4.93	3.03	0.26	0.17
	Tissue dissection	3	5.56	2.96	2.29	0.21	0.09
	Mean	5	5.59	3.75	2.59	0.22	0.13
Liver	Autoradiography	2	6.82	6.22	3.07	0.26	0.15
	Tissue dissection	3	4.37	2.35	1.74	0.17	0.08
	Mean	5	5.35	3.90	2.27	0.21	0.11
Muscle	Autoradiography	2	1.00	1.13	0.88	0.07	0.03
	Tissue dissection	3	1.53	1.73	1.12	0.06	0.06
	Mean	5	1.32	1.48	1.02	0.06	0.05
Pancreas	Autoradiography	2	2.40	3.20	2.75	0.22	0.16
Ovary	Autoradiography	2	6.83	5.21	2.15	0.23	0.18
Bone marrow	Autoradiography	2	6.61	7.05	3.99	0.70	0.34
Thymus	Autoradiography	2	3.23	2.75	1.37	0.41	0.18
Uterus	Autoradiography	2	4.06	7.70	3.02	0.22	0.18
Thyroid	Autoradiography	2	31.50	32.20	157.00	75.70	229.00
Femur	Tissue dissection	3	3.21	2.53	2.07	0.31	0.11
Whole body	Autoradiography	2	3.29	4.44	3.01	0.40	0.33

found in the spleen (C_{max} = 35.8) and is similar to what was observed for the spleen in normal mice. However, the C_{max} in BCL1 tumor-bearing mice occurred 3 h after injection, whereas C_{max} occurred at 1 h after injection in normal mice. In addition, although the %ID/g was higher in the mesenteric lymph nodes (C_{max} = 8.2) than in most other tissues, the levels of radioactivity were not as high as in the lymph nodes of normal mice (C_{max} = 17.7). This may be because the lymph nodes of BCL1 tumor-bearing mice were often greatly enlarged relative to those of normal mice, possibly indicating an edematous state (mean weight, 14.8 mg in BCL1 tumor-bearing mice, compared with 8.8 mg in normal mice). The larger weight lowers the concentration when %ID is divided by the weight of the tissue. As in normal mice, high levels of radioactivity were found in the stomach (C_{max} = 11.8) of BCL1 tumor-bearing mice, whereas the kidneys, liver, muscle, heart, duodenum, and femur all had a relatively low %ID/g.

The %ID/mL values for blood, plasma, and urine (TCA-precipitable activity) for BCL1 tumor-bearing mice are listed in Table 4. The plasma half-life is 2.65 h and agrees well with the plasma half-life of ^{125}I-BLyS in normal mice and the reported plasma half-life of unlabeled BLyS. Although the half-life of ^{125}I-BLyS is similar in normal and BCL1 tumor-bearing mice, the volume of distribution is greater in tumor-bearing mice (225 mL/kg) than in normal mice (150 mL/kg). This is demonstrated by the observation that the values for %ID/g in blood and plasma at each time point are lower in tumor-bearing mice than in normal mice. The increased volume may be due to a larger number of BLyS-receptor–positive cells in the tumor-bearing mice and suggests that tumor binding removes BLyS from the plasma compartment.

The ratios of the area under the %ID/g curve for the tissues, AUC_{tissue}, to the AUC_{blood} are listed in Table 5. Spleen and lymph node had the highest AUC_{tissue}/

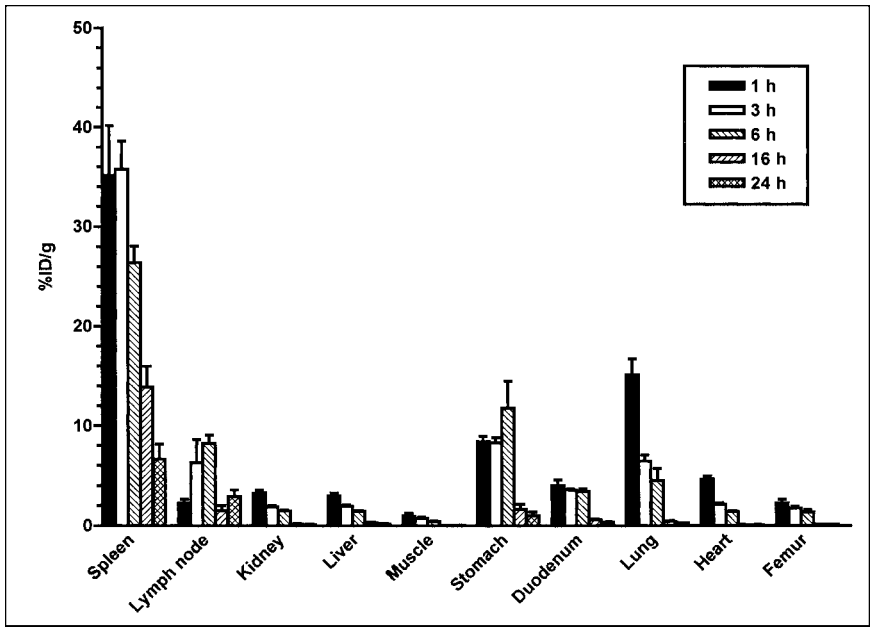

FIGURE 3. %ID/g after intravenous injection of 50 μg/kg of ^{125}I-BLyS into BCL1 tumor-bearing BALB/c mice. BCL1 tumor-bearing female BALB/c mice were injected intravenously with ^{125}I-BLyS at 50 μg/kg, and biodistribution was determined by tissue dissection method at 1, 3, 6, 16, and 24 h after injection. Error bars represent SEM.

AUC_{blood}, with values of 11.00 and 2.89, respectively. In contrast, the AUC ratios for the lung, kidney, and liver were 1.49, 0.44, and 0.46, respectively, demonstrating the greater specificity of ^{125}I-BLyS for lymphoid tissues. The AUC ratio in the spleen for BCL1 tumor-bearing mice was greater than in normal mice (ratio = 6.53). This could be due to a larger number of BLyS-receptor–positive cells in the spleens of BCL1 tumor-bearing mice, as well as a lower AUC in blood. The AUC ratio in the lymph node was lower for BCL1 tumor-bearing mice than for normal mice (ratio = 3.35). The comparatively lower value in lymph nodes may indicate edematous lymph nodes. The stomach also had a high AUC ratio (2.70), presumably because of free ^{125}I.

QWBA images of BCL1 tumor-bearing mice are shown in Figure 4. Radioactivity in the BCL1 enlarged spleens is high at early times and is still evident at 24 h, indicating that BCL1 tumors are capable of binding ^{125}I-BLyS. Lymph nodes also appear enlarged, compared with lymph nodes in normal animals. As was seen in normal animals, lymph nodes and gut-associated lymphoid tissue were positive for radioactivity, demonstrating the ability of BLyS to target B cell–rich tissues, and high levels of radioactivity were also found in the thyroid, stomach, and submandibular salivary gland.

Biodistribution in J558 Tumor-Bearing Mice

To assess the ability of ^{125}I-BLyS to distribute to tumors in nonlymphoid tissues, we used a second tumor model in which the murine plasmacytoma, J558, was injected into the subcutaneous space on the hind flank of BALB/c mice. Similar J558 models have been used in studies of cytokine-based cancer therapies (*33*,*34*). This model is particularly well suited for studies of ^{125}I-BLyS because the tumor expresses BLyS receptors and its growth in the subcutane-

TABLE 4
%ID (TCA-Precipitable)/mL of Blood, Plasma, and Urine After Intravenous Injection of 50 μg/kg of ^{125}I-BLyS in BCL1 Tumor-Bearing BALB/c Mice (±SEM)

Time	Blood	Plasma	Urine
5 min	16.80 ± 0.66	33.30 ± 4.25	1.31
30 min	11.40 ± 0.75	23.30 ± 1.67	5.23 ± 1.59
1 h	6.92 ± 0.77	13.90 ± 1.43	2.94 ± 0.42
3 h	2.83 ± 0.25	6.56 ± 0.50	6.49 ± 1.75
6 h	1.25 ± 0.10	1.56 ± 0.22	5.89 ± 0.74
16 h	0.08 ± 0.02	0.09 ± 0.02	0.63 ± 0.06
24 h	0.06 ± 0.01	0.04 ± 0.01	0.66 ± 0.13

Urine values represent activity present only at specified time point, not cumulative excretion.

TABLE 5
Ratio of AUC_{tissue} to AUC_{blood} in BCL1 Tumor-Bearing Mice

Tissue	AUC	AUC_{tissue}/AUC_{blood}
Blood	50.00	1.00
Spleen	552.00	11.00
Lymph node	145.00	2.89
Stomach	135.00	2.70
Lung	74.60	1.49
Duodenum	46.60	0.93
Liver	23.20	0.46
Heart	23.10	0.46
Kidney	21.80	0.44
Femur	18.90	0.38
Muscle	6.66	0.13

SOCIETY OF NUCLEAR MEDICINE

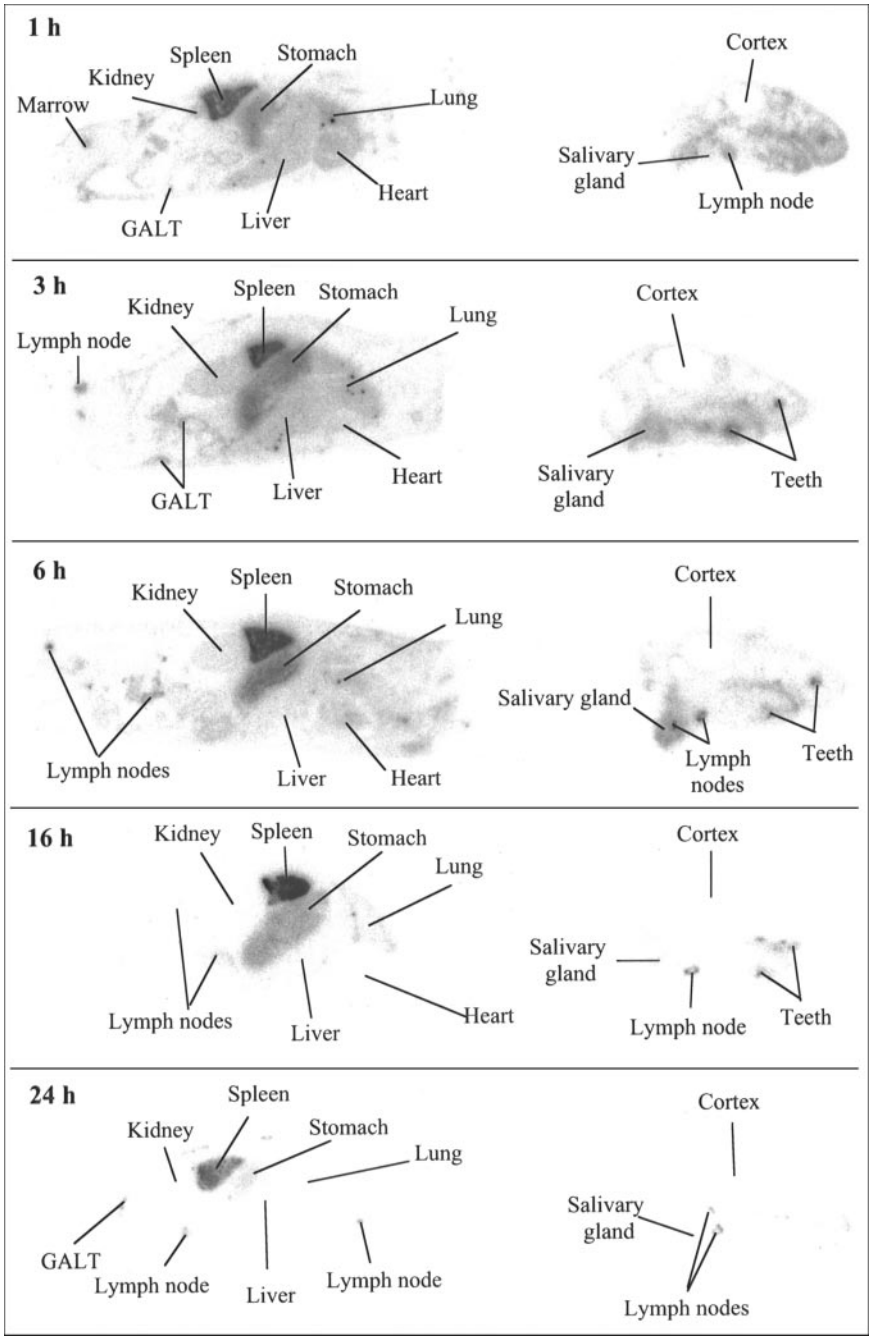

FIGURE 4. QWBA after intravenous injection of 50 μg/kg of ^{125}I-BLyS into BCL1 tumor-bearing BALB/c mice. BCL1 tumor-bearing female BALB/c mice were injected intravenously with ^{125}I-BLyS at 50 μg/kg and were frozen for QWBA at 1, 3, 6, 16, and 24 h after injection. Images were contrast-enhanced for display purposes only. GALT = gut-associated lymphoid tissue.

ous space mirrors that of lymphomas that arise in nonlymphoid compartments.

The %ID/g of ^{125}I-BLyS in J558 tumor-bearing mice at 6 and 24 h after injection is shown in Figure 5 for the tissues collected by dissection. The highest %ID/g was found in the spleen (C_{max} = 40.2), followed by the mesenteric lymph nodes (C_{max} = 24.0) and the J558 tumor (C_{max} = 15.3). The values for C_{max} in the spleen and lymph node are similar to those observed in normal mice injected with ^{125}I-BLyS. In addition, good uptake in the J558 tumor demonstrated the ability of radiolabeled BLyS to target plasma cell tumors. As in normal and BCL1 tumor-bearing mice, high levels of radioactivity were also found in the stomach (C_{max} = 15.2) of J558 tumor-bearing mice. The %ID/mL of blood, plasma, and urine at 6 and 24 h after injection were similar to levels observed in normal mice.

QWBA images obtained from J558 tumor-bearing mice are shown in Figure 6. The images confirm the localization of ^{125}I-BLyS to the spleen, lymph nodes, and tumor and also demonstrate targeting to gut-associated lymphoid tissue. The relatively uniform distribution of radioactivity in the J558 tumor indicates that ^{125}I-BLyS is able to penetrate

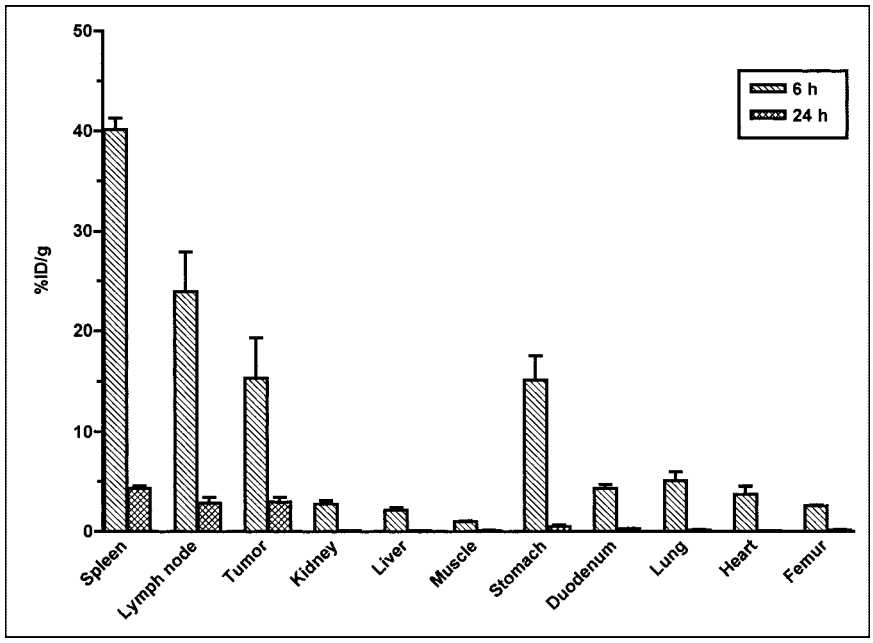

FIGURE 5. %ID/g after intravenous injection of 50 μg/kg of ^{125}I-BLyS into J558 tumor-bearing BALB/c mice. J558 tumor-bearing female BALB/c mice were injected intravenously with ^{125}I-BLyS at 50 μg/kg, and biodistribution was determined by tissue dissection at 6 and 24 h after injection. Error bars represent SEM.

throughout the tumor. As in normal mice, high levels of radioactivity were also found in the thyroid, stomach, and submandibular salivary gland.

Dosimetry

Human radiation dose estimates for ^{131}I-labeled BLyS developed from the normal mouse biodistribution data are listed in Table 6. With the exception of the thyroid, the highest radiation dose is predicted to be to the spleen (1.2 mGy/MBq) after administration of ^{131}I-BLyS. The dose to the bone marrow, an organ sensitive to radiation, is estimated to be 0.15 mGy/MBq (0.55 cGy/mCi).

DISCUSSION

These studies show the rapid and specific targeting of radioiodinated BLyS to lymphoid tissues and B cell tumors. After intravenous injection of ^{125}I-BLyS in mice, tissues that have a high proportion of B cells, such as spleen, lymph nodes, and gut-associated lymphoid tissue, had relatively high uptake and exposure (AUC), demonstrating the specificity of BLyS for B cells. High levels of radioactivity were also seen in the thyroid, stomach contents, and salivary glands, consistent with the expected distribution of free iodide (*30*). Lung uptake at 1 h was higher than that in lymph nodes but then declined in parallel to the plasma concentration, suggesting that lung exposure was due to the high blood volume in this tissue. Other tissues, including kidneys, liver, muscle, heart, duodenum, and femur, all had relatively low values for %ID/g. Radiolabeled BLyS also showed localization to spleens containing BCL1 lymphoma cells and subcutaneously implanted J558 plasma cell tumors.

The biodistribution of BLyS in mice differs considerably from that of other radiolabeled proteins, including antibodies directed against B cells. Illidge et al. (*35*) measured the biodistribution of radioiodinated anti-B cell monoclonal antibodies in mice bearing BCL1 tumors. The maximal uptake of the anti-CD22 antibody in the spleen, where BCL1 tumor cells migrate to and proliferate, was ~15 %ID/g, compared with ~35 %ID/g for BLyS. The antibody also had much higher maximal values in liver (15%–20 %ID/g) and kidney (10%–15 %ID/g) than did BLyS (~5 %ID/g). By 24 h, the radioactivity in liver and kidney had decreased to 2–7 %ID/g for the anti-B cell antibodies, but after radiolabeled BLyS injection, these organs were almost completely cleared of radioactivity at 24 h (<0.2 %ID/g).

Buschbaum et al. (*36*) studied the biodistribution of radioiodinated anti-J5 antibody in athymic mice in which human B cell Namalwa tumors were implanted subcutaneously. The tumor-to-blood ratio ranged from 0.7 to 1.2 over a 7-d period, with the maximum occurring 4 d after injection. By contrast, in the subcutaneous J558 tumor, BLyS achieved tumor-to-blood ratios of 4.1 and 50 at 6 and 24 h, respectively. In comparison with other proteins, such as Fab′ fragments and streptavidin, that are of comparable molecular weight to BLyS (molecular weight = 52 kDa), BLyS has far lower kidney accumulation. For example, Colcher et al. (*37*) found that the Fab′ of the antibody B6.2 has a maximal kidney uptake of 132 %ID/g at 0.5 h in athymic mice. The values at 1, 6, and 24 h were 41, 33, and 2.9 %ID/g, respectively, whereas for BLyS, the values are only 5.6, 2.6, and 0.13 %ID/g. Wilbur et al. (*38*) found that ^{131}I-labeled streptavidin had a ~20 %ID/g uptake in the

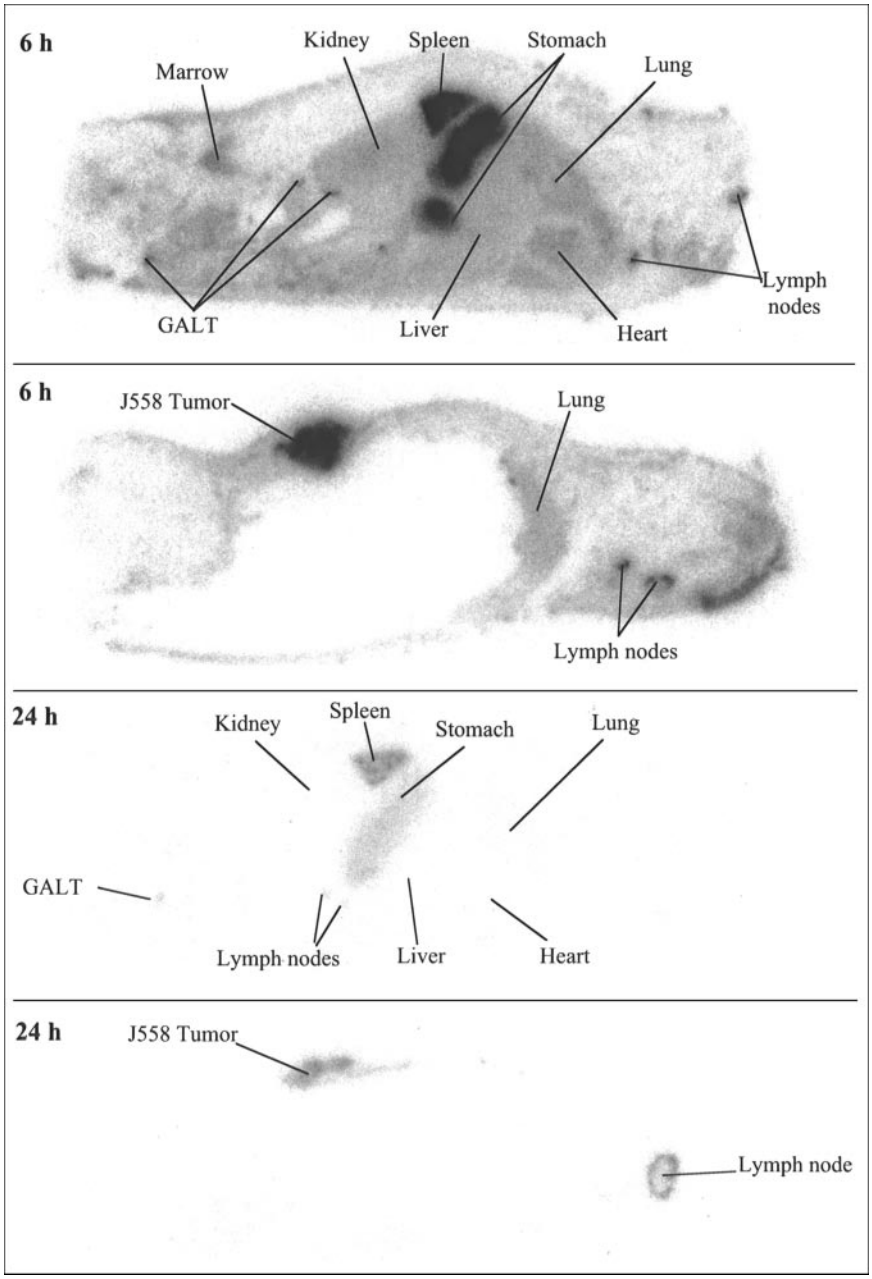

FIGURE 6. QWBA after intravenous injection of 50 μg/kg of ^{125}I-BLyS into J558 tumor-bearing BALB/c mice. J558 tumor-bearing female BALB/c mice were injected intravenously with ^{125}I-BLyS at 50 μg/kg and were frozen for QWBA at 6 and 24 h after injection. Two cross-sections taken at different depths from same animal are shown for each time point to illustrate distribution both at level of subcutaneous tumor and at level of most major organs. Images were contrast-enhanced for display purposes only. GALT = gut-associated lymphoid tissue.

kidneys of athymic mice 4 h after injection, and this concentration persisted through 48 h.

Because the bone marrow is the most radiosensitive organ, radioimmunotherapy protocols are generally limited by dose to the marrow. Meredith et al. (*39*) have reviewed several radioimmunotherapy trials, and they estimate that the maximally tolerated dose to the bone marrow after ^{131}I therapy is 185 cGy. Based on the dose estimates for ^{131}I-BLyS in humans (Table 6), the bone marrow is predicted to receive 0.15 mGy/MBq. Although the human dose estimates for BLyS radiolabeled with ^{131}I are based on extrapolation from mouse biodistribution data for the ^{125}I analog and must be interpreted cautiously, the predictions suggest that the maximally tolerated dose of ^{131}I-BLyS will be approximately 12 GBq (324 mCi).

In addition to its distinct biodistribution, the ability of BLyS to bind to multiple myeloma cells and to target and penetrate a subcutaneous plasmacytoma in a murine model suggests that radiolabeled BLyS could potentially offer a new therapeutic option for a disease with few other treatment options. In contrast to BLyS receptors, the CD20 antigen is expressed on the plasma cells in only a fraction of multiple myeloma patients, and expression can be weak and heterogeneous (*25*), limiting the use of anti-CD20 antibodies in this indication. Taken together, the unique biodistribution, pharmacokinetics, and receptor distribution of ra-

TABLE 6
Human Organ Radiation Doses for ^{131}I-Labeled BLyS

Target organ	mGy/MBq	cGy/mCi
Adrenals	1.4E−01	5.0E−01
Brain	1.1E−01	3.9E−01
Breasts	1.0E−01	3.7E−01
Gallbladder wall	1.3E−01	4.9E−01
Lower large intestine wall	1.3E−01	4.7E−01
Small intestine	1.3E−01	4.8E−01
Stomach	2.7E−01	9.9E−01
Upper large intestine wall	1.3E−01	4.8E−01
Heart wall	1.8E−01	6.8E−01
Kidneys	1.4E−01	5.2E−01
Liver	1.3E−01	4.8E−01
Lungs	2.2E−01	8.0E−01
Muscle	1.1E−01	4.2E−01
Ovaries	1.6E−01	5.7E−01
Pancreas	1.6E−01	5.8E−01
Red marrow	1.5E−01	5.5E−01
Bone surfaces	1.5E−01	5.5E−01
Skin	9.5E−02	3.5E−01
Spleen	1.2E+00	4.3E+00
Testes	1.1E−01	4.0E−01
Thymus	1.1E−01	4.1E−01
Thyroid	1.1E+01	4.1E+01
Urinary bladder wall	1.2E−01	4.6E−01
Uterus	1.3E−01	4.8E−01
Total body	1.2E−01	4.6E−01
Effective dose equivalent	5.5E−01	2.0E+00
Effective dose	7.5E−01	2.8E+00

diolabeled BLyS provide a rationale for future studies on human populations with a variety of B cell malignancies.

CONCLUSION

Radiolabeled BLyS showed specific and rapid targeting to lymphoid tissues and 2 different B cell tumors in mice. The relatively short half-life and low exposure of this cytokine to normal organs suggest that radiolabeled BLyS may offer advantages over radioimmunotherapy with monoclonal antibodies in certain clinical settings. These data provide preclinical support for future studies of the pharmacokinetics and biodistribution of radiolabeled BLyS in human populations with B cell malignancies.

ACKNOWLEDGMENTS

The authors thank Dr. Ralph Alderson, Dr. Viktor Roschke, Victor Kao, and Naran Bao for providing the tumor-bearing animals; Drs. Albert Chan and Corinne Bensimon at MDS Nordion for radiolabeling BLyS; Drs. Wendy Halpern, Susan Wojcik, and James Fikes for help with histologic evaluations; Hsiu-Ling Lin for technical assistance; and Dr. David Hilbert for helpful comments on the manuscript. Financial support for this work was provided by Human Genome Sciences, Inc.

REFERENCES

1. Moore PA, Belvedere O, Orr A, et al. BLyS: member of the tumor necrosis factor family and B lymphocyte stimulator. *Science.* 1999;285:260–263.
2. Schneider P, MacKay F, Steiner V, et al. BAFF, a novel ligand of the tumor necrosis factor family, stimulates B cell growth. *J Exp Med.* 1999;189:1747–1756.
3. Tribouley C, Wallroth M, Chan V, et al. Characterization of a new member of the TNF family expressed on antigen presenting cells. *Biol Chem.* 1999;380:1443–1447.
4. Mukhopadhyay A, Ni J, Zhai Y, Yu GL, Aggarwal BB. Identification and characterization of a novel cytokine, THANK, a TNF homologue that activates apoptosis, nuclear factor-kappaB, and c-Jun NH2-terminal kinase. *J Biol Chem.* 1999;274:15978–15981.
5. Shu HB, Hu WH, Johnson H. TALL-1 is a novel member of the TNF family that is down-regulated by mitogens. *J Leukoc Biol.* 1999;65:680–683.
6. Do RK, Hatada E, Lee H, Tourigny MR, Hilbert D, Chen-Kiang S. Attenuation of apoptosis underlies B lymphocyte stimulator enhancement of humoral immune response. *J Exp Med.* 2000;192:953–964.
7. Parry TJ, Riccobene TA, Strawn SJ, et al. Pharmacokinetics and immunological effects of exogenously administered recombinant human B lymphocyte stimulator (BLyS) in mice. *J Pharmacol Exp Ther.* 2001;296:396–404.
8. Gross JA, Dillon SR, Mudri S, et al. TACI-Ig neutralizes molecules critical for B cell development and autoimmune disease: impaired B cell maturation in mice lacking BLyS. *Immunity.* 2001;15:289–302.
9. Schiemann B, Gommerman JL, Vora K, et al. An essential role for BAFF in the normal development of B cells through a BCMA-independent pathway. *Science.* 2001;293:2111–2114.
10. Mackay F, Woodcock SA, Lawton P, Amet al. Mice transgenic for BAFF develop lymphocytic disorders along with autoimmune manifestations. *J Exp Med.* 1999;190:1697–1710.
11. Khare SD, Sarosi I, Xia XZ, et al. Severe B cell hyperplasia and autoimmune disease in TALL-1 transgenic mice. *Proc Natl Acad Sci USA.* 2000;97:3370–3375.
12. Gross JA, Johnston J, Mudri S, et al. TACI and BCMA are receptors for a TNF homologue implicated in B-cell autoimmune disease. *Nature.* 2000;404:995–999.
13. Thompson JS, Schneider P, Kalled SL, et al. BAFF binds to the tumor necrosis factor receptor-like molecule B cell maturation antigen and is important for maintaining the peripheral B cell population. *J Exp Med.* 2000;192:129–135.
14. Xia XZ, Treanor J, Senaldi G, et al. TACI is a TRAF-interacting receptor for TALL-1, a tumor necrosis factor family member involved in B cell regulation. *J Exp Med.* 2000;192:137–143.
15. Yan M, Marsters SA, Grewal IS, Wang H, Ashkenazi A, Dixit VM. Identification of a receptor for BLyS demonstrates a crucial role in humoral immunity. *Nat Immunol.* 2000;1:37–41.
16. Shu HB, Johnson H. B cell maturation protein is a receptor for the tumor necrosis factor family member TALL-1. *Proc Natl Acad Sci USA.* 2000;97:9156–9161.
17. Wu Y, Bressette D, Carrell JA, et al. Tumor necrosis factor (TNF) receptor superfamily member TACI is a high affinity receptor for TNF family members APRIL and BLyS. *J Biol Chem.* 2000;275:35478–35485.
18. Marsters SA, Yan M, Pitti RM, Haas PE, Dixit VM, Ashkenazi A. Interaction of the TNF homologues BLyS and APRIL with the TNF receptor homologues BCMA and TACI. *Curr Biol.* 2000;10:785–788.
19. Thompson JS, Bixler SA, Qian F, et al. BAFF-R, a newly identified TNF receptor that specifically interacts with BAFF. *Science.* 2001;293:2108–2111.
20. Yan M, Wang H, Chan B, et al. Activation and accumulation of B cells in TACI-deficient mice. *Nat Immunol.* 2001;2:638–643.
21. Kanakaraj P, Migone TS, Nardelli B, et al. BLyS binds to B cells with high affinity and induces activation of the transcription factors NF-kappaB and ELF-1. *Cytokine.* 2001;13:25–31.
22. Briones J, Timmerman JM, Hilbert DM, Levy R. BLyS and BLyS receptor expression in non-Hodgkin's lymphoma. *Exp Hematol.* 2002;30:135–141.
23. Kaminski MS, Estes J, Zasadny KR, et al. Radioimmunotherapy with iodine (131)I tositumomab for relapsed or refractory B-cell non-Hodgkin lymphoma: updated results and long-term follow-up of the University of Michigan experience. *Blood.* 2000;96:1259–1266.
24. Witzig TE, White CA, Wiseman GA, et al. Phase I/II trial of IDEC-Y2B8 radioimmunotherapy for treatment of relapsed or refractory CD20(+) B-cell non-Hodgkin's lymphoma. *J Clin Oncol.* 1999;17:3793–3803.
25. Treon SP, Shima Y, Grossbard ML, et al. Treatment of multiple myeloma by antibody mediated immunotherapy and induction of myeloma selective antigens. *Ann Oncol.* 2000;11:107–111.
26. Waldmann TA, Strober W. Metabolism of immunoglobulins. *Prog Allergy.* 1969;13:1–110.
27. Kirschner AS, Ice RD, Beierwaltes WH. Radiation dosimetry of ^{131}I-19-iodocho-

lesterol: the pitfalls of using tissue concentration data [reply to letter]. *J Nucl Med.* 1975;16:248–249.
28. Sparks R, Aydogen B. Comparison of the effectiveness of some common animal data scaling techniques in estimating human radiation dose. In: *Proceedings from the Sixth International Radiopharmaceutical Dosimetry Symposium, May 7–10, 1996.* Oak Ridge, TN: Oak Ridge Institute for Science and Education; 1996:705–716.
29. Stabin MG. MIRDOSE: personal computer software for internal dose assessment in nuclear medicine. *J Nucl Med.* 1996;37:538–546.
30. Regoeczi E. *Iodine Labeled Plasma Protein*. Vol II, Part B. Boca Raton, LA: CRC Press; 1987:48–71.
31. Brudevold F, Tehrani A, Cruz R. The relationship among the permeability to iodide, pore volume, and intraoral mineralization of abraded enamel. *J Dent Res.* 1982;61:645–648.
32. Knapp MR, Jones PP, Black SJ, Vitetta ES, Slavin S, Strober S. Characterization of a spontaneous murine B cell leukemia (BCL1). I. Cell surface expression of IgM, IgD, Ia, and FcR. *J Immunol.* 1979;123:992–999.
33. Qin Z, Blankenstein T. Tumor growth inhibition mediated by lymphotoxin: evidence of B lymphocyte involvement in the antitumor response. *Cancer Res.* 1995;55:4747–4751.
34. Cayeux S, Beck C, Dorken B, Blankenstein T. Coexpression of interleukin-4 and B7.1 in murine tumor cells leads to improved tumor rejection and vaccine effect compared with single gene transfectants and a classical adjuvant. *Hum Gene Ther.* 1996;7:525–529.
35. Illidge TM, Cragg MS, McBride HM, French RR, Glennie MJ. The importance of antibody-specificity in determining successful radioimmunotherapy of B-cell lymphoma. *Blood.* 1999;94:233–243.
36. Buchsbaum DJ, Sinkule JA, Stites MS, et al. Localization and imaging with radioiodine-labeled monoclonal antibodies in a xenogeneic tumor model for human B-cell lymphoma. *Cancer Res.* 1988;48:2475–2482.
37. Colcher D, Bird R, Roselli M, et al. In vivo tumor targeting of a recombinant single-chain antigen-binding protein. *J Natl Cancer Inst.* 1990;82:1191–1197.
38. Wilbur DS, Stayton PS, To R, et al. Streptavidin in antibody pretargeting: comparison of a recombinant streptavidin with two streptavidin mutant proteins and two commercially available streptavidin proteins. *Bioconjug Chem.* 1998;9:100–107.
39. Meredith R. Scoring of radionuclide therapy endpoints: normal organ toxicity, tumor response and patient outcome. *Cancer Biother Radiopharm.* 2002;17:83–99.

SOCIETY OF NUCLEAR MEDICINE